Available online at www.sciencedirect.com
SCIENCE DIRECT®
PERGAMON
International Journal of Heat and Mass Transfer 46 (2003) 4191–4199
International Journal of HEAT and MASS TRANSFER
www.elsevier.com/locate/ijhmt

Use of porous baffles to enhance heat transfer in a rectangular channel

Kang-Hoon Ko, N.K. Anand *

Department of Mechanical Engineering, Texas A&M University, College Station, TX 77843-3123, USA

Received 5 August 2002; received in revised form 28 April 2003

Abstract

An experimental investigation was carried out to measure module average heat transfer coefficients in uniformly heated rectangular channel with wall mounted porous baffles. Baffles were mounted alternatively on top and bottom of the walls. Heat transfer coefficients and pressure loss for periodically fully developed flow and heat transfer were obtained for different types of porous medium (10, 20, and 40 pores per inch (PPI)) with two window cut ratios ($B_h/D_h = 1/3$ and 2/3) and two baffle thickness to channel hydraulic diameter ratios ($B_t/D_h = 1/3$ and 1/12). Reynolds number (Re) was varied from 20,000 to 50,000. To compare the effect of foam metal baffle, the data for conventional solid-type baffle were obtained for ($B_t/D_h = 1/3$). The maximum uncertainties associated with module Nusselt number and friction factor were 5.8% and 4.3% respectively. The experimental procedure was validated by comparing the data for the straight channel with no baffles ($B_h/D_h = 0$) with those in the literature [Publications in Engineering, vol. 2, University of California, Berkeley, 1930, p. 443; Int. Chem. Eng. 16 (1976) 359]. The use of porous baffles resulted in heat transfer enhancement as high as 300% compared to heat transfer in straight channel with no baffles. However, the heat transfer enhancement per unit increase in pumping power was less than one for the range of parameters studied in this work. Correlation equations were developed for heat transfer enhancement ratio and heat transfer enhancement per unit increase in pumping power in terms of Reynolds number.

Keywords: Porous media; Heat transfer enhancement; Porous baffles

1. Introduction

The use of serpentine type or baffled type channels is one of the commonly used passive heat transfer enhancement strategies in single-phase internal flows. Accordingly, the study of fluid flow and heat transfer in serpentine channels has received considerable attention [1,2]. This passive heat transfer enhancement strategy has been used for various types of industrial applications such as shell-and-tube type heat exchangers, electronic cooling devices, thermal regenerators, internal cooling systems of gas turbine blades, and labyrinth seals for turbo-machines. Periodically positioned baffles in baffled channels and periodic turns in serpentine channels periodically interrupt hydrodynamic and thermal boundary layers. Downstream of each baffle (or turns in serpentine channels) the flow separates, re-circulates, and impinges on the wall. Flow impingement and fin effect are the main reasons for heat transfer enhancement in such channels. Due to periodicity in geometry the flow and heat transfer will never reach fully developed state. However, in modules far from the channel entrance flow and heat transfer will be periodically fully developed [3,4]. While the use of solid baffles results in significant heat transfer enhancement the associated increase in pressure drop and higher local thermal stress at the root of the baffle is of concern. Thus warranting the exploration of the use of porous baffles to enhance heat transfer while keeping the pressure drop to a minimum. The advantages of using porous baffles are: (1) it has higher surface area to volume ratio, which will increase the dispersion of the heat drastically; (2) due to its

* Corresponding author.
E-mail address: nkanand@mengr.tamu.edu (N.K. Anand).

0017-9310/$ - see front matter
doi:10.1016/S0017-9310(03)00251-5

Nomenclature

A	flow cross-sectional area
A_s	area of a plate
B_h	baffle height
B_p	baffle pitch
B_t	baffle thickness
C_p	specific heat at constant pressure
D_h	hydraulic diameter ($4A/P$)
f	friction factor
H	channel height
h	heat transfer coefficient
K	thermal conductivity, permeability ($Q/[A(\Delta P/L)]$ in Darcy's equation)
L	distance between pressure taps
$\dot{m}$	mass flow rate of air
Nu	Nusselt number
$\overline{Nu}_p$	average plate Nusselt number
$\overline{Nu}_m$	average module Nusselt number
$\overline{Nu}_s$	Nusselt number for fully developed flow in a straight channel
$\overline{Nu^+}$	heat transfer enhancement ratio ($\overline{Nu}_{m,pdf}/\overline{Nu}_s$)
$\overline{Nu^*}$	heat transfer performance ratio ($\overline{Nu^+}/(f_{m,pdf}/f_s)^{1/3}$)
P	perimeter, pressure
PPI	pores per linear inch in each direction
Q	amount of heat applied, flow rate
Q_{loss}	amount of heat lost to the ambient
Re	Reynolds number based on channel hydraulic diameter ($\rho U D_h/\mu$)
T_{in}	module inlet temperature of air
$\overline{T}_b$	bulk temperature of air
$\overline{T}_w$	average mean wall temperature
U	average air velocity
V_f	volume of fluid
V_{total}	total volume
W	channel width

Greek symbols

β	ratio of the orifice plate diameter to the pipe diameter
ε	porosity (V_f/V_{total})
ρ	density
μ	dynamic viscosity
Δ	difference

Subscripts

f	fluid
i	baffle index
p	plate
pdf	periodically fully developed flow
m	module
w	wall

structural stiffness and light weight, it can be used for thermal management in aerospace applications, and (3) its nature of forcing uniform distribution of flow will homogenize the thermal dispersion of the surface, which will reduce local thermal stress.

Koh and Stevens [5] demonstrated the enhancement of cooling effectiveness by using porous materials in a coolant passage subject to constant heat flux. Wall temperature in circular passage was dropped dramatically and the temperature of coolant almost doubled. Kuo and Tien [6] presented numerical results for fully packed bed with a foam material to enhance liquid forced convection cooling in low Reynolds number ranges ($Re = 2000$–6000) with discrete heat sources. They found that the heat transfer increased between 2 and 4 times and the enhancement was due to the dispersion of heat in the solid matrix and the heat transfer enhancement was pronounced at high flow rates and for large permeability. Rachedi and Chikh [7] numerically studied forced convection cooling in the presence of porous inserts in electronic devices. Results showed that the temperature dropped down by half. Hwang and Chao [8] showed that the smaller size of pore density can decrease the entrance length and increase the local Nusselt number in their packed bed experiment using sintered material. They introduced two-equation model to overcome heat transfer over prediction of conventional one equation model and showed the existence of non-equilibrium thermal condition between the fluid and the solid matrix. Recently, Kim et al. [9] experimentally investigated an asymmetrically heated packed bed filled with foam materials. Consideration was given to foam materials. They developed correlation equations for Nusselt number for different foam materials as function of Darcy number. Hwang and Liou [10] found that the thermal performance was best when the ratio between vacant area and solid area (open area ratio) in the ribs was 44%. Using this configuration, Liou and Chen [11] experimentally studied turbulent heat transfer and fluid flow in a rectangular channel with perforated ribs. Consideration was given to both attached (to wall) and detached ribs. Perforated ribs were made up of aluminum. Their study indicated that the highest Nusselt number to be around three (3) times larger than that for a corresponding channel without ribs. Hwang [12] conducted experiments to study turbulent heat transfer and fluid flow in a porous baffled channel. The porous baffles were mounted on top and bottom walls in a

staggered manner. In addition, experiments were conducted with solid baffles for the sake of comparison. Consideration was given to two different baffle heights and Reynolds number was varied between 20,000 and 50,000. In this study thermocouple wires were mounted along the channel center-line to measure the local heat transfer. Accordingly, heat transfer data was reported only along the center-line of the channel. In addition, Hwang [12] measured turbulent intensity and velocity profile using hot wire anemometry. His study showed that the porous baffled channel have a significantly lower friction factor.

The objective of the present work was to conduct experiments to measure module average Nusselt number and friction factor for flow in a staggered porous baffled channel. It is clear from reviewing the literature the work of Hwang [12] is only one similar to the one presented in this paper. However, the present work differs from that of Hwang [12] in following ways: (a) in the present study the test section was heated along all four walls whereas in the previous case [12] only the top wall was heated; (b) Hwang [12] reported local heat transfer data along the centerline of the channel whereas in the present work the focus is on measuring module average Nusselt number; (c) in the present work experiments were conducted with three (3) different pore densities (viz.: 10 PPI, 20 PPI, and 40 PPI) whereas in the previous case [12] the porosity was held constant at 0.42; (d) the present set of experiments were conducted with porous baffles with two different thickness (1 and 0.25 in.) whereas in the previous case [12] the baffle thickness was not varied; (e) the results of the present work is a representative of a three dimensional flow situation (aspect ratio $H/W = 1$) whereas the results of the previous case better represents a two-dimensional situation (aspect ratio $H/W = 0.25$); and (f) in the present work the material used for baffle is a aluminum foam material manufactured using a process patented by ERG Aerospace Inc., CA (see Fig. 1) whereas in the previous case [12] porous baffles were made of sintered bronze beads. Thus the scope of the present study is very different than that of Hwang [12]. In the following sections, description of the experimental test setup, associated instrumentation, experimental procedure, uncertainty analysis, range of independent parameters, and representative results will be presented.

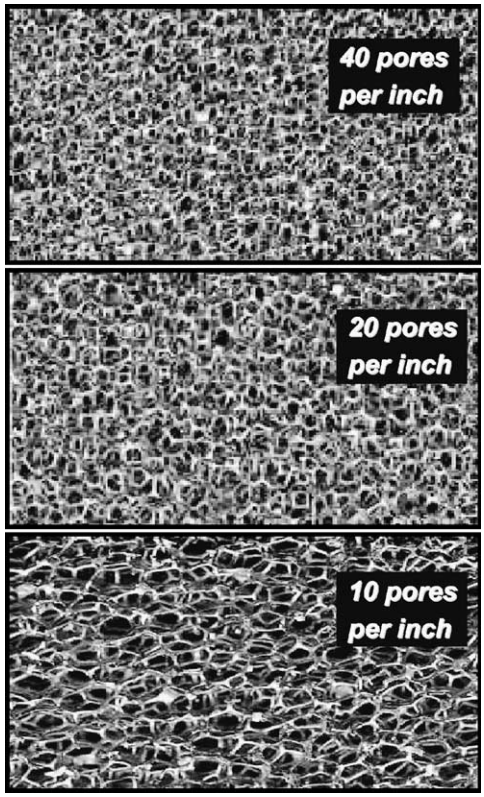

Fig. 1. Aluminum foam structure.

2. Experimental setup

Fig. 2 shows the schematic diagram of experimental setup. It is consisted of four major components: (a) the flow system, (b) baffled test section, (c) heating unit, and (d) measurement system. The flow system was operated in a suction mode and oriented horizontally. Air drawn through the channel entrance, flows through baffled test section, the mixing chamber, flow meter, and exhausted by two serially linked 1.5 hp blowers. The connection between blowers and test setup were made with a flexible high pressure vacuum tube to minimize vibration. A control valve was used to control the flow rate. An orifice flow meter was used downstream of the mixing chamber to measure air flow rate. A mixing chamber was located downstream of the test section to stabilize the flow. The open test loop had an entrance length of 48 in. Long entry region was provided so that flow would be fully developed as it enters the baffled section. Fig. 3 shows the details of the test section. The test section has a 3 in. $\times$ 3 in. ($H \times W$) square cross-sectional unit and a length of 36 in. (L_1). Baffles were located in a staggered manner by mounting baffles alternately on top and bottom walls. Baffles were firmly glued to the walls using thermal epoxy. The distance between two successive baffles (pitch, B_p) was 3 in. and was maintained constant throughout this study. To facilitate the flow to develop as it enters the test section two unheated baffles were set in front of the heated baffles. Entrance length is set to be long enough to make sure that the flow is fully developed at the entrance to the test section.

The test section was built with 40 (3 in. $\times$ 3 in.) copper plates. T type (copper–constantine) thermocouples

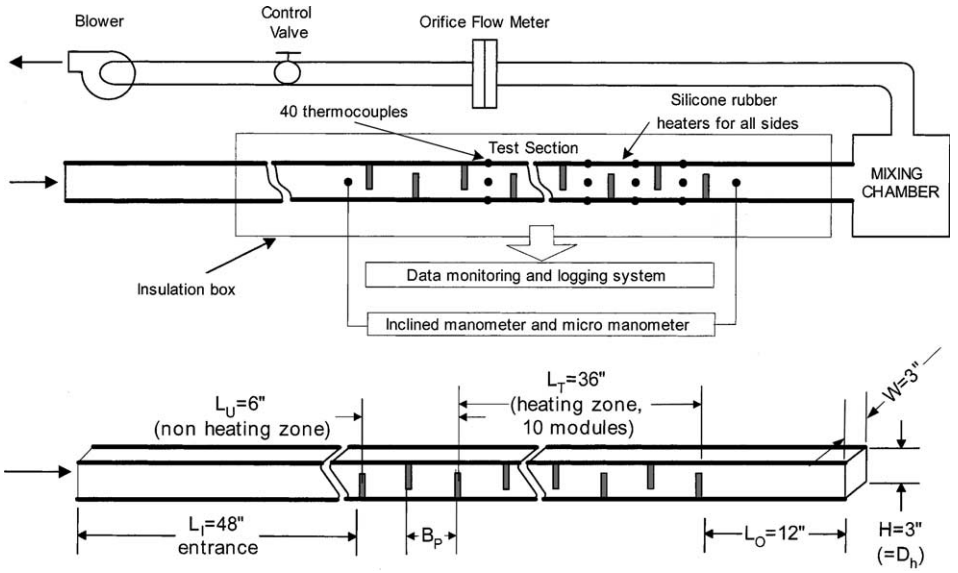

Fig. 2. Schematic diagram of the experimental setup.

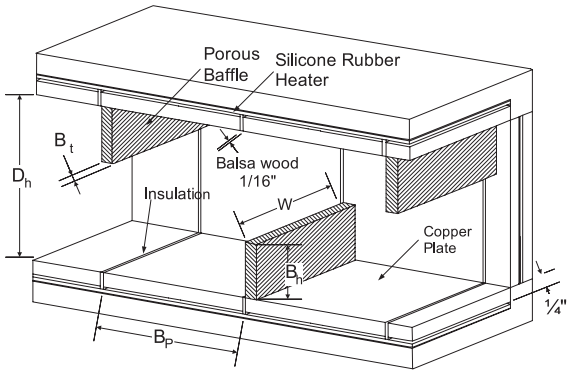

Fig. 3. Schematic of the test section.

with Teflon insulation were carefully inserted in drilled holes underneath the surfaces of the each plate to measure the average temperature of plates. Silver paint was used to ensure proper contact between the thermocouples and the copper plates. These contacts were electronically checked by using Ohm meter. Each of the plates in the stream-wise direction was separated by balsa wood to ensure the insulation from each other. Back side of each plate was attached to silicone rubber heater with a thin layer of highly conductive silicon. The square copper plate channel was well insulated on the outside by using four (4) inch thick fiberglass insulation and placed in a wooden box. Silicone rubber heaters from each side were parallel1y connected and powered through a transformer. The temperature of the test section was controlled by a Watlow auto-tuning controller.

3. Instrumentation

The copper–constantine thermocouples were calibrated against the Fischer thermal bath with a variation of 0.1 °F or less over the range of operating temperatures in this study. The range of Reynolds numbers examined in this study was, $Re = 20,000–50,000$. The flow Reynolds numbers were calculated by measuring the flow rate. Flow rates were measured by orifice meter using the 1.5 in. orifice plate made by Daniel. The U type water manometer and inclined oil manometer were used to measure pressure drop across the orifice plate. The pressure taps were located at a distance of 1.5 in. on either side of the test section. The pressure drop in a straight channel (with no baffles) was measured with a micro-manometer for higher accuracy and an inclined manometer was used for the baffled channel. Total power applied to the test section was calculated using the voltage and current measured using a multi-meter, which had a factory precision of 2.5% and 2% respectively. Various temperatures were monitored using a computer-controlled data acquisition system. The maximum temperature was limited and controlled by a Watlow auto-controller until the system reached steady state for more than 10 min with less than 0.5 °F variations in temperatures.

4. Data reduction

The Reynolds number based on the hydraulic diameter is evaluated as

$$Re = \frac{\rho U D_h}{\mu} = \frac{4\dot{m}}{\pi \mu D_h} \quad (1)$$

where, U and $\dot{m}$ are the average velocity and the mass flow rate of air at the test section.

The friction factor in a periodically fully developed baffled channel flow can be determined by measuring the pressure drop across the flow channel and the average velocity of the air. The average friction factor can then be calculated from

$$f = \frac{(\Delta P/L)D_h}{\rho U^2/2} \quad (2)$$

where, L denotes the distance between pressure taps. The average heat transfer coefficient for the ith copper segment ($i = 1$ to 40) is

$$h_i = \frac{Q_i}{A_s(\overline{T}_w - \overline{T}_b)} = \frac{Q_p - Q_{loss,i}}{A_s(\overline{T}_w - \overline{T}_b)} \quad (3)$$

where, A_s is the area of the inner surface of the plate segment, $\overline{T}_w$ is average wall temperature, $\overline{T}_b$ is bulk temperature calculated from an energy balance, $\overline{T}_b = \overline{T}_{in} + Q_i/(\dot{m}C_p)$ and Q_i is the actual amount of heat applied to the ith module, Q_i is estimated by subtracting the heat loss ($Q_{loss,i}$) from the electrical input. Thus the average Nusselt number for each plate is calculated as

$$\overline{Nu}_p = \frac{h_i D_h}{K_f} \quad (4)$$

Each module is made of four plates i.e. top, bottom, left, and right. Then average module Nusselt number ($\overline{Nu}_m$) can be calculated as the weighted average of Nusselt numbers ($\overline{Nu}_p$) for each plate. The weighting factors are areas of each plate.

5. Uncertainty analysis

A detailed uncertainty analysis was conducted. The variables measured are temperature, pressure drop, and heat applied to each module. The uncertainty associated with each variable is the square root sum of the squares of precision and bias errors. The bias error was found to be negligibly small compared to the precision errors accordingly, bias errors associated with each variable was neglected. The precision error associated with heat applied to each module stems from the voltage and current measurements. Precision errors associated with voltage and current measurements were provided by the instrument manufacturer and were 2% and 2.5% respectively. The measurement of airflow rate using the orifice plate involved measurement of pressure drop and discharge coefficient. For the current configuration of the $\beta = 0.6$ (ratio of the orifice diameter to the pipe diameter) and Reynolds number range of 20,000–50,000 the maximum error for discharge coefficient is reported as 0.6% [13,14]. Considering maximum uncertainty of pressure, the uncertainty of mass flow from orifice meter is estimated to be less than 1.3%. The propagation equation of Kline and McClintock [15] and ANSI guide to the Expression of Uncertainty in Measurement [16] were referred to calculate uncertainties associated with friction factor (f) and module Nusselt number ($\overline{Nu}_m$) and the associated intermediate variables. The maximum uncertainty associated with the module Nusselt number measurement was 5.8%. The uncertainty associated friction factor was 4.3%.

6. Independent parameters

All experiments were conduced with air accordingly, Prandtl number was fixed at 0.7 and adjustments were made to account for variation of properties with the temperature. Consideration was given to a single value of channel aspect ratio ($H/W = 1$). While the porosity (ε) of the aluminum foam had a constant value of 0.92 and consideration was given to three different pore densities viz.: 10 PPI, 20 PPI, and 40 PPI, where, PPI stands for pores per linear inch. The flow Reynolds number was varied between 20,000 and 50,000.

However, due to excessive pumping power requirement for the solid baffle case experiments were limited to $Re = 3 \times 10^4$. Experiments were conducted with two different baffle thickness values viz. $B_t/D_h = 1/3$ and 1/12. Measurements were made with porous and solid baffles. In order to benchmark and validate the data, measurements were made for the case of straight channel with no baffles ($B_h/D_h = 0$). Consideration was given to a fixed value of baffle pitch ($B_p = 3$ in.). The scope of experimental study included two different baffle heights and they were $B_h/D_h = 1/3$ and 2/3. The ranges of independent parameters explored in this study are summarized in Table 1.

7. Results and discussion

The current experimental procedure was validated by making heat transfer measurements for flow through a straight channel without any baffles ($B_h/D_h = 0$). The variation of average Nusselt number with Reynolds number for fully developed flow in straight channels is shown in Fig. 4. In this figure the current experimental data is compared against the correlations available in the literature. The average Nusselt number for fully developed flow in a straight channel was compared with results obtained from correlation of Gnielinski [17] and Dittus–Boelter [18]. The maximum difference for average Nusselt Number obtained in the present work and those correlations in the literature [17,18] is 5.9%.

Fig. 5 shows module Nusselt number ($\overline{Nu}_{m,i}$) for the pore density of 20 PPI, and baffle height ratio of

Table 1
Test parameters

B_h/D_h	$B_t/D_h = 1/3$				$B_t/D_h = 1/12$			
	10 PPI	20 PPI	40 PPI	Solid	10 PPI	20 PPI	40 PPI	Solid
1/3	X	X	X	X	X	X	X	
2/3	X	X	X	X	X	X	X	

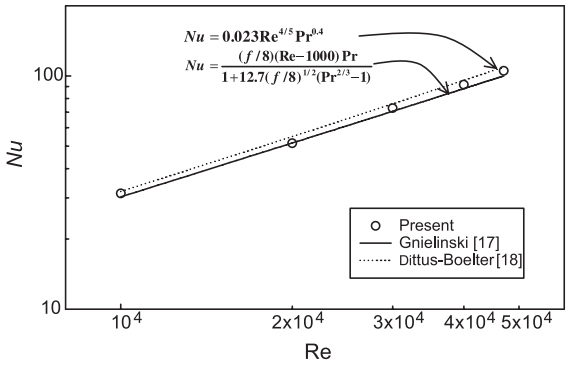

Fig. 4. Validation of heat transfer experiments.

$B_h/D_h = 1/3$. In the previous work of Berner et al. [3], it was found that the flow periodically fully develops downstream of fourth (4th) module for thin solid baffle. Considering the baffle thickness and pore density is different from solid baffle, it is expected that the entry length for flow through porous baffle channel is longer than for the flow through the solid baffle channel. It is evident from Fig. 5 that the variation pattern of average module Nusselt number repeats itself downstream of seventh (7th) module (including baffles in unheated

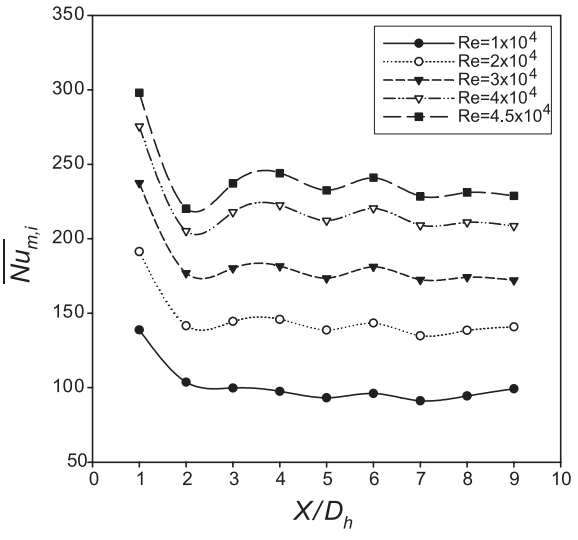

Fig. 5. Average module Nusselt number for 20 PPI, $B_h/D_h = 1/3$.

sections). Thus clearly establishing the existence periodically fully developed heat transfer in such porous baffled channel flows. As expected the average module Nusselt number decreases in the downstream direction and increases with increase in Reynolds number.

The effectiveness of using porous baffles was evaluated by studying ratio of average module Nusselt number ($\overline{Nu_{m,pdf}}$) for periodically fully developed flow and the average Nusselt number ($\overline{Nu_s}$) for fully developed flow in a straight channel ($B_h/D_h = 0$). Henceforth, this ratio will be referred to as the heat transfer enhancement ratio ($\overline{Nu^+} = \overline{Nu_{m,pdf}}/\overline{Nu_s}$). The variation of this heat transfer enhancement ratio ($\overline{Nu^+}$) with Reynolds number for various cases is shown in Fig. 6 for a fixed value of $B_h/D_h = 1/3$. For the case of $B_h/D_h = 1/3$ and for entire range of independent parameters examined in this study, the heat transfer enhancement ratio ($\overline{Nu^+}$) is greater than unity (Fig. 6a), signifying that the use of porous baffles over plain straight channel is advantageous. In some cases the heat transfer enhancement ratio is as high as 300%. As expected the solid baffles perform better than the porous baffles from heat transfer point of view with an enhancement ratio as high as 390%. The heat transfer enhancement ratio decreases with increase in Reynolds number. This is attributed to the fact that at higher *Re* values the turbulent effects play much more dominant role than the baffle effects such as impingement and fin effects. For a fixed pore density the heat transfer enhancement ratio increases with increase in baffle thickness. It is evident that the ratio $\overline{Nu^+}$ for thicker baffle ($B_t/D_h = 1/3$) is consistently higher than those for thinner baffles ($B_t/D_h = 1/12$). This behavior is expected as the thicker baffle provides greater convection and diffusion heat transfer area. Kuo and Tien's [6] results showed that heat transfer enhancement is greater at higher flow rates and larger permeabilities (K). According to the material properties (Table 2) provided by Kim et al. [9] and the present results showed (Figs. 6 and 7) that heat transfer enhancement is inversely proportional to the permeability for both high (present) and low flow rates [9]. This behavior is consistent with the fact that for a fixed baffle thickness the heat transfer enhancement ratio ($\overline{Nu^+}$) increases with increase in pore density. Accordingly, the baffles with the pore density of 40 PPI perform the best. It is also interesting to see that the variations in $\overline{Nu^+}$ with pore density for thick baffles ($B_t/D_h = 1/3$) is greater compared to those for thinner

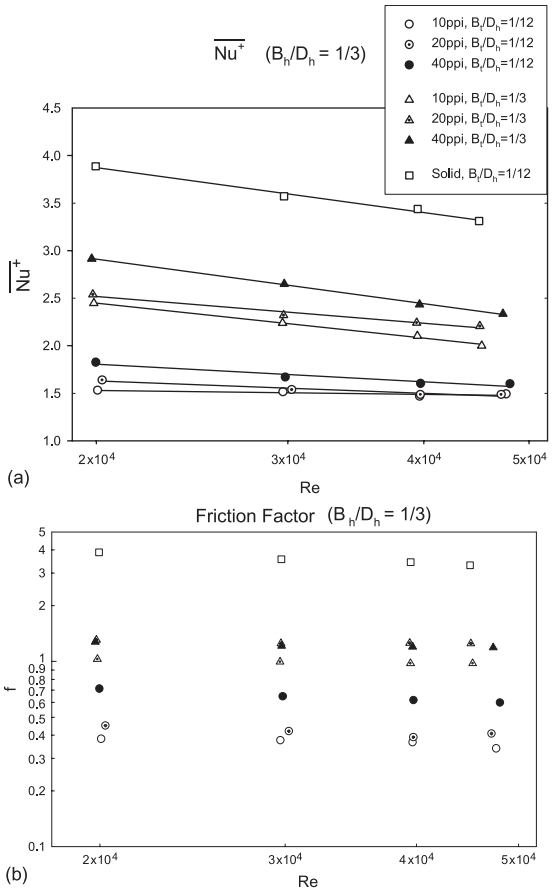

Fig. 6. Heat transfer and friction factor for $B_h/D_h = 1/3$: (a) heat transfer enhancement ratio, (b) friction factor.

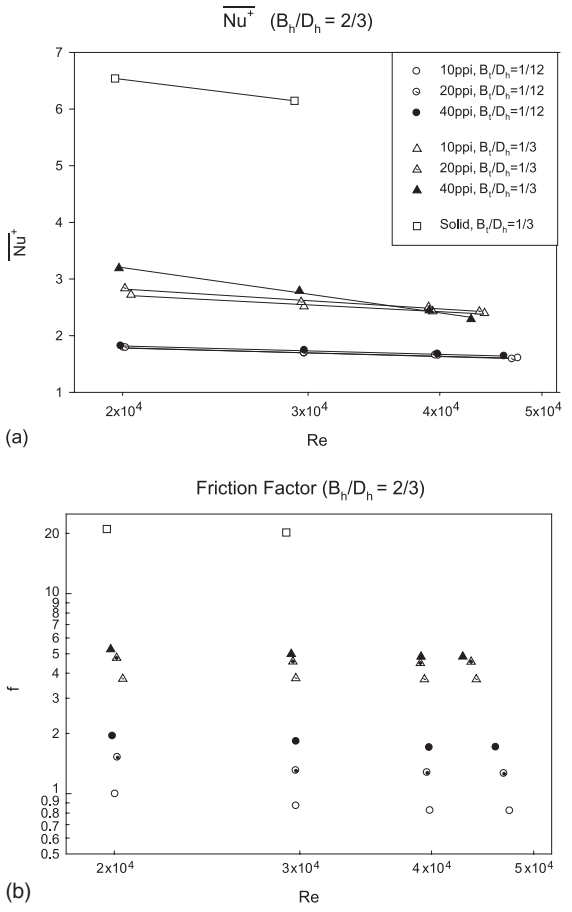

Fig. 7. Heat transfer and friction factor for $B_h/D_h = 2/3$: (a) heat transfer enhancement ratio, (b) friction factor for $B_h/D_h = 2/3$.

Table 2
Thermo-physical parameters for aluminum foams [9]

Pore density (PPI)	10	20	40
Materials	Al-6101	Al-6101	Al-6101
Porosity, e	0.92	0.92	0.92
Permeability, K (m^2)	1.04E−7	0.76E−7	0.51E−7

baffles ($B_t/D_h = 1/12$). But from Fig. 7, it is evident that for taller ($B_h/D_h = 2/3$) and thicker ($B_t/D_h = 1/3$) baffles as flow rates increase the effect of pore density on $\overline{Nu^+}$ diminishes. This behavior can be explained using the Darcy's equation [19]: $Q = K \times A \times \Delta P/L$. For a fixed flow rate, if the pressure drop across the baffle is large then the effect of permeability is small. On the other hand when the flow rate is small and the pressure drop across the baffle is small then the effect of permeability is large. The friction factor decreases slightly with increase in Re (Fig. 6b). As expected the solid baffles has the highest friction factor. In general for a fixed Re, the friction factor increases with increase in pore density. Accordingly, for the case of thicker baffles ($B_t/D_h = 1/3$) with pore density of 40 PPI has the highest friction factor. This behavior is attributed to the fact that the contact surface area between the fluid and the solid increases with increase in pore density thus increasing the amount of hydraulic resistance, but this behavior comes into play only at lower flow rates and shorter baffles heights. This behavior is more distinct for thicker ($B_t/D_h = 1/3$) and taller baffles ($B_h/D_h = 2/3$) as shown in Figs. 6 and 7. Also, it is evident from Figs. 6 and 7 that the effect of pore density is more dominant in the lower Reynolds number range.

The effectiveness of using porous baffles can also be studied evaluating the heat transfer performance ratio. The heat transfer performance ratio is defined as the ratio of heat transfer enhancement to unit increase in pumping power ($\overline{Nu^*} = \overline{Nu^+}/(f_{m,pdf}/f_s)^{1/3}$). In this ratio the friction factors are raised to the one-third power as the pumping power is proportional to the one-third power of the friction factor. For applications wherein the pumping power is of concern the ratio $\overline{Nu^*}$ should

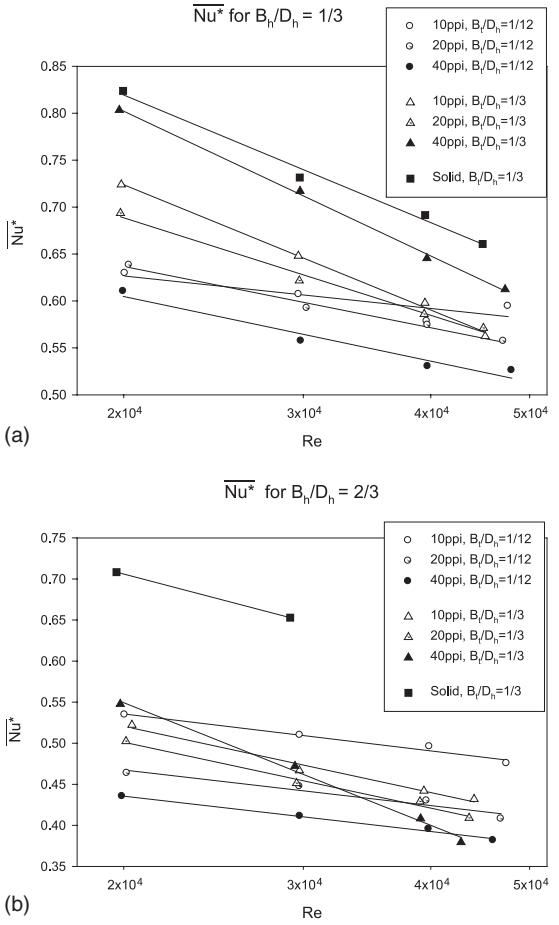

Fig. 8. Heat transfer performance: (a) heat transfer performance $B_h/D_h = 1/3$, (b) heat transfer performance $B_h/D_h = 2/3$.

greater than unity (1). It is evident from Fig. 8 that none of the data points satisfy this condition. But there are several applications where pumping power is not scarce as in the case of automobile or offshore drilling applications. In these cases space may be premium thus making the use of lightweight porous baffles are very attractive. As expected the heat transfer ratio ($\overline{Nu^*}$) decreases with increase in Re. This behavior is attributed to the fact that at higher Reynolds number turbulent effects prevail over enhancement due to porous baffles. As in the previous case (Figs. 6 and 7) the heat transfer ratio ($\overline{Nu^*}$) for thicker baffle ($B_t/D_h = 1/3$) are higher. This is because of the fact that greater heat transfer area is associated with thicker baffles. For both baffles thickness cases ($B_t/D_h = 1/3$ and 1/12), baffles with the pore density of 40 PPI performs better at lower Reynolds number.

Based on the experimental data correlations for heat transfer enhancement ratio ($\overline{Nu^+}$) and heat transfer performance ratio ($\overline{Nu^*}$) were developed in terms of Reynolds number by using the method of least squares. The correlations were of the form $\overline{Nu} = c_0 + c_1 \times Re \times 10^{-6}$. In Table 3 values for C_0 and C_1 for various cases are given.

8. Summary

Experiments were conducted to study heat transfer enhancement in a rectangular channel by using a porous baffle made up of aluminum foam. Baffles were mounted on bottom and top walls in a staggered fashion. Experiments were conducted in Reynolds number range of 20,000–50,000. The maximum uncertainties associated with average module Nusselt number and friction factor were 5.8% and 4.3% respectively. The experimental procedure was validated by comparing the data for the straight channel with no baffles ($B_h/D_h = 0$) with those in the literature [17,18]. Experiments showed that the flow and heat transfer to reach periodically fully developed state downstream of the seventh module. For the

Table 3
Correlation coefficients for Nusselt numbers $\overline{Nu} = c_0 + c_1 \times Re \times 10^{-6}$

			$B_t/D_h = 1/12$			$B_t/D_h = 1/3$			Solid
			10 PPI	20 PPI	40 PPI	10 PPI	20 PPI	40 PPI	1/3
$B_h/D_h = 1/3$	$\overline{Nu^+}$	c_0	1.56	1.78	1.94	2.77	2.75	3.30	4.28
		c_1	−1.81	−6.95	−7.80	−17.13	−12.62	−20.93	−21.73
$B_h/D_h = 1/3$	$\overline{Nu^*}$	c_0	0.65	0.70	0.66	0.84	0.93	0.93	0.93
		c_1	−1.48	−3.08	−2.92	−6.19	−3.24	−6.89	−6.17
$B_h/D_h = 2/3$	$\overline{Nu^+}$	c_0	1.90	1.98	1.95	2.96	3.13	3.94	7.36
		c_1	−6.39	−8.78	−6.83	−13.17	−16.25	−38.55	−41.77
$B_h/D_h = 2/3$	$\overline{Nu^*}$	c_0	0.57	0.51	0.47	0.59	0.57	0.69	0.82
		c_1	−2.06	−2.16	−1.99	−3.63	−3.73	−7.21	−5.87

Pore density in PPI, Baffle thickness (B_t/D_h).

range of independent parameters examined in this study following conclusive statements can be made. The heat transfer enhancement ratio ($\overline{Nu^+}$) decreases with increase in Reynolds number and increases with increase in pore density. The heat transfer enhancement ratio reaches a maximum value of 300% for the range of parameters studied in this investigation. The heat transfer enhancement ratio was found to be higher for taller ($B_h/D_h = 2/3$) and thicker ($B_t/D_h = 1/3$) baffles. The ratio of heat transfer enhancement to per unit increase in pumping power was less than one. The friction factor slightly decreased with increase in Reynolds number, and increased with baffle thickness and pore density. Based on the experimental data, correlations for heat transfer enhancement ratio ($\overline{Nu^+}$) and heat transfer performance ratio ($\overline{Nu^*}$) were developed in terms of Reynolds number.

Acknowledgement

This work was supported in part by the Texas A&M University Energy Resources Program (ERP-99-25).

References

[1] J.M. Choi, N.K. Anand, Heat-transfer in a serpentine channel with a series of right-angle turns, Numer. Heat Transfer, Part A 23 (1993) 189–210.
[2] J.M. Choi, N.K. Anand, S.C. Lau, R.T. Kukreja, Heat (Mass) transfer in a serpentine channel with right-angled turns, ASME J. Heat Transfer 118 (1996) 211–213.
[3] C. Berner, F. Durst, D.M. McEligot, Flow around baffles, ASME J. Heat Transfer 106 (1984) 743–749.
[4] S.H. Kim, N.K. Anand, Turbulent heat-transfer between a series of parallel plates with surface-mounted discrete heat-sources, ASME J. Heat Transfer 116 (1994) 577–587.
[5] J.C.Y. Koh, R.L. Stevens, Enhancement of cooling effectiveness by porous materials in coolant passage, ASME J. Heat Transfer 97 (1975) 309–311.
[6] S.M. Kuo, C.L. Tien, Heat transfer augmentation in a foam-material filled duct with discrete heat sources, Thermal Phenomena in the Fabrication and Operation of Electronic Components: I-THERM'88, Inter Society Conference, Los Angeles, CA, USA, 1988, pp. 87–91.
[7] R. Rachedi, S. Chikh, Enhancement of electronic cooling by insertion of foam materials, Heat Mass Transfer 37 (2001) 371–378.
[8] G.J. Hwang, C.H. Chao, Heat transfer measurement and analysis for sintered porous channels, ASME J. Heat Transfer 116 (1994) 456–464.
[9] S.Y. Kim, B.H. Kang, J.H. Kim, Forced convection from aluminum foam materials in an asymmetrically heated channel, Int. J. Heat Mass Transfer 44 (2001) 1451–1454.
[10] J.J. Hwang, T.M. Liou, Augmented heat transfer in a rectangular channel with permeable ribs mounted on the wall, ASME J. Heat Transfer 116 (1994) 912–920.
[11] T.M. Liou, S.H. Chen, Turbulent heat and fluid flow in a passage disturbed by detached perforated ribs of different heights, Int. J. Heat Mass Transfer 41 (1998) 1795–1806.
[12] J.J. Hwang, Turbulent heat transfer and fluid flow in a porous-baffled channel, AIAA J. Thermophys. Heat Transfer 11 (1997) 429–436.
[13] R.W. Fox, A.T. McDonald, Introduction to Fluid Mechanics, 4th ed., John Wiley, New York, 1992, pp. 380–382.
[14] International Organization of Standards (ISO 5167-1), Measurement of fluid flow by means of pressure differential devices, Part 1: Orifice plates, nozzles, and Venturi tubes inserted in circular cross-section conduits running full, Reference number: ISO 5167-1:1991(E); 1991, p. 10.
[15] S.J. Kline, F.A. McClintock, Describing uncertainties in single-sample experiments, Mech. Eng. 75 (1953) 3–8.
[16] American National Standards Institute, U.S. Guide to the Expression of Uncertainty in Measurement, ANSI/NCSL Z540-2-1997, 1997, pp. 9–22.
[17] V. Gnielinski, New equations for heat and mass-transfer in turbulent pipe and channel flow, Int. Chem. Eng. 16 (1976) 359–368.
[18] F.W. Dittus, L.M.K. Boelter, Publications in Engineering, vol. 2, University of California, Berkeley, CA, 1930, p. 443.
[19] B. Jacob, Dynamics of Fluids in Porous Media, Dover Publications, New York, 1988.